NUMERICAL TREATMENT OF WELLS IN 2D HYBRID GRIDS

Giovani Cerbato

giovani.cerbato@sinmec.ufsc.br

Fernando S. V. Hurtado

fernando@sinmec.ufsc.br

Gustavo Gondran Ribeiro

ggrbill@sinmec.ufsc.br

Taisa Beatriz Pacheco

taisa@sinmec.ufsc.br

António Fábio Carvalho da Silva

afabio@sinmec.ufsc.br

Clovis R. Maliska

maliska@sinmec.ufsc.br

Federal University of Santa Catarina, SINMEC Laboratory, Florianópolis, Brasil.

Abstract. *The near-well regions require special attention in reservoir simulation due to the pronounced pressure gradients in those regions. Hence, the large pressure variation near the wells are rarely well captured with the commonly employed grid refinement. One of the leading goals of adopting hybrid grids is to capture the flow behavior in those regions with more accuracy. This paper presents two different approaches to deal with that situation. The first one treats the well-reservoir interface as a grid boundary. Then, as the grid gets closer to the well, it is demanded a severe refinement in the radial direction. The second approach employs a well model with the purpose of avoiding extremely refined grid. A single phase flow problem with a known well pressure value was solved in order to test the feasibility of these two approaches with several two-dimensional hybrid grids. The results are compared with a reference solution, which, regardless of also being numerical, was solved in a highly refined grid, especially in the near-well area.*

Keywords: *well, hybrid grids, grid refinement, well model*

1 INTRODUCTION

The near-well regions require special attention in the numerical formulation for reservoir simulation. The main characteristic of the fluid flow in those regions is the strong variation of the physical parameters, specially pressure, in a relative small area. Therefore, an extremely refined grid would be needed in order to capture the large pressure gradients in the vicinity of the wells. However, this approach is not feasible for the corner point grids usually employed to discretize the reservoirs. The rigid topological structure of these grids complicates the procedure of employing a local refinement (LGR) and, concurrently, remaining the rest of the grid unchanged.

The combination of grids with different topological structure, generating hybrid grids, makes that procedure more feasible. This approach is exposed in the section 2 as an alternative for treating the near-well region. However, the most commonly alternative employed to overcome the mentioned difficulties is the use of the so-called well models. The adopted strategy to determine the well indexes values for the hybrid grids employed here is described in section 3. The objective of the current study is to determine the most convenient way to represent the wells in the discrete model. The hybrid grids employed in the tests have the configuration presented in Fig. 1. For the analyzed 2D situation, the adjacent region of the well is discretized by a polar grid and it is inserted in a portion of the reservoir corner point grid. The transition between these two grids is done by a polygonal grid.

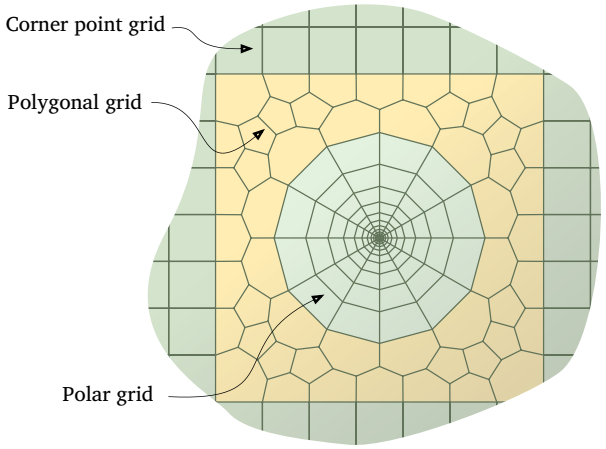

Figure 1: Configuration of the 2D hybrid grid.

2 APPROACH 1: RADIAL REFINEMENT AROUND WELLS

The arrangement of the hybrid grid allows a progressive radial refinement of the polar grid, so that the pressure gradient near of the well can be captured accurately. It is clear that this will lead to a larger number of cells in the polar grid. However, in transitional and corner-point portions, the number of cells will not change.

In the approach 1, as illustrated in Fig. 2, the well surface is represented as one more boundary in the discrete model. Depending on the well operational conditions, a Dirichlet or a Neumann condition should be prescribed. If the surface pressure is known, the former is applied. On the other hand, if the flow crossing the surface is known, the latter is employed.

Aiming to achieve acceptable numerical results with this approach, the radial spacing of the grid cells near the well must be small enough in order to capture accurately the gradients. Determining the appropriate size of this spacing is one of the goals in the current study.

However, in order to avoid an excessive increasing of the number of cells, it is convenient to consider a gradual increasing in the radial spacing of the polar grid, as shown in Fig. 2. Regarding the grids employed in the tests presented below, an exponential growth of the radial spacing was considered. More specifically, the radial coordinates of the vertices in the polar grid were determined by the expression

$$r_k = Ae^{B\cdot k} + C\,, \tag{1}$$

where k is an index associated with each constant radius in the polar grid, while A, B and C are constants which values are determined in order to satisfy geometric constraints. It is known that the pressure in the vicinity of a well varies in a logarithm way, in relation to the radial coordinate (Peaceman, 1978). Therefore, if a polar grid with the radial spacing described by the Eq. (1) is employed, then an approximately uniform pressure variation between the cells is expected.

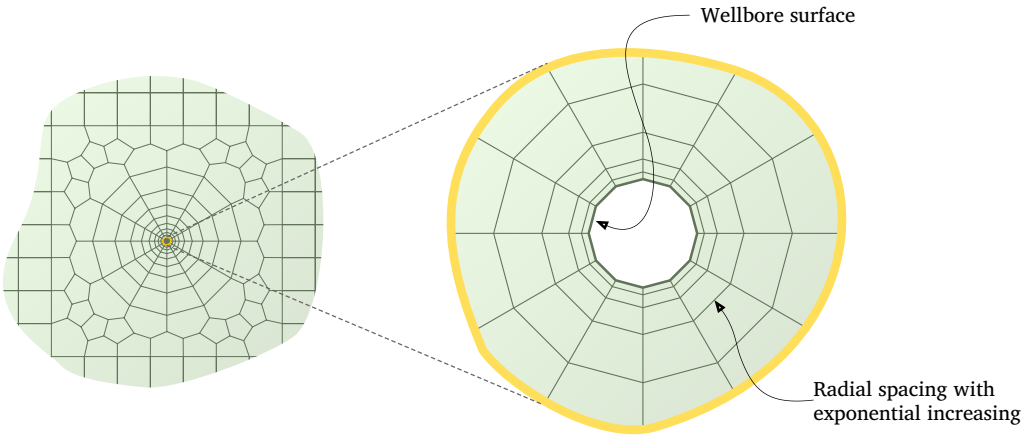

Figure 2: Discrete representation of the wellbore surface in approach 1.

3 APPROACH 2: USING A WELL MODEL

Another alternative to consider the influence of wells in the flow model is to adopt a well model. Although the polar grid allows more detailed solutions in the vicinity of the well, it may increase the number of equations beyond a reasonable limit, due to the requirement of a highly refined grid. In these situations, the most advantageous approach is to employ a well model, as done when conventional grids are used. A brief review on the main concepts associated with these well models are now presented.

The well models are usually defined considering a steady state flow model. However, the model expressions can be directly generalized for applications in more complicated reservoir simulation involving multiphase flows (Peaceman, 2003). The most common expression that defines a well model is

$$q = \lambda\,\mathrm{WI}\left(P_\mathrm{p} - P_\mathrm{w}\right), \tag{2}$$

where q is the flow rate between the reservoir and the well, P_{w} and P_{p} are the wellbore pressure and the pressure associated with the cell that contains the well, respectively, and λ is the mobility. For a single-phase flow, the mobility is defined as the inverse of the viscosity μ. The fundamental parameter in the Eq. (2) is WI, referred as productivity index or well index. This parameter depends on the geometric characteristics of the well, the grid surrounding the well, and also on the permeability in that region. The main task of a well model is to determine an appropriate WI value for a given geometrical configuration of the well in relation to the grid surrounding it.

The Peaceman well model (Peaceman, 1978) is one of the most employed in reservoir simulation. The original model is based on the analytical solution for the pressure variation in a radial, single-phase and steady state flow. The porous medium is considered isotropic and homogeneous, discretized with a regular Cartesian grid. Subsequently, the same author has extended the model to more complex cases, for instance, employing grids with rectangular cells and/or anisotropic media (Peaceman, 1983) and also non centered well inside the cell and cells with more than one well (Peaceman, 1990). Since these procedures are not directly applicable to the polar grid, employed to discretize the near well region in the present case, a more general approach was adopted. It is described in the next subsection.

3.1 Well index determination

In this study, the numerical methodology considered to discretize the fluid flow equations is able to treat unstructured grids with arbitrary permeabilities. Therefore, it was decided to include a procedure that determines well indexes with the same generality, as was originally proposed by Aavatsmark and Klausen (2003). The method description adapted to 2D problems is presented below.

The physical situation considered in the model derivation is illustrated in Fig. 3(a), in which the wellbore radius r_w is located at the origin of an infinite two-dimensional domain. For a steady state, the single-phase and incompressible flow to the well is described by the equations

$$\boldsymbol{\nabla}\cdot\mathbf{v} = 0\,, \tag{3}$$

$$\mathbf{v} = -\lambda\,\mathbf{K}\boldsymbol{\nabla}P\,, \tag{4}$$

subjected to the following conditions at the interface between the well and the reservoir

$$P\,\big|_{r=r_w} = P_{\mathrm{w}}\,, \tag{5}$$

$$\int_{r=r_w} \mathbf{v}\cdot\mathrm{d}\mathbf{S} = q\,. \tag{6}$$

In the vicinity of the well, it is assumed a homogeneous medium. However, the permeability can be described by an anisotropic tensor $\mathbf{K}$. For the mentioned conditions, it is possible to determine an analytical solution for the pressure variation about the well [1], which is

$$P = P_{\mathrm{w}} + \frac{q}{2\pi\lambda\,h\,(K_{\mathrm{X}}\,K_{\mathrm{Y}})^{1/2}}\,\ln\!\left(\frac{r^*}{\bar{r}_w}\right), \tag{7}$$

[1] The derivation process of this solution is quite laborious. The details can be found in Peaceman (1983).

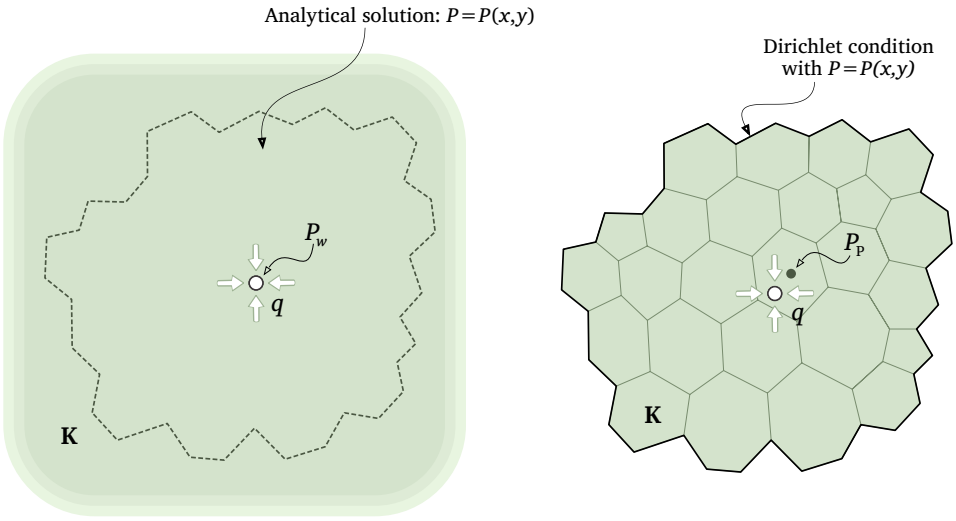

(a) Problem specification (b) Auxiliary problem

Figure 3: Auxiliary problem employed to determine the well index.

where h is the reservoir thickness. The parameters r^* and $\bar{r}_w$ are defined, considering the X and Y axes whose origin is located in the center of the well, as

$$r^* = \sqrt{\left(\frac{K_Y}{K_X}\right)^{1/2} X^2 + \left(\frac{K_X}{K_Y}\right)^{1/2} Y^2}, \tag{8}$$

$$\bar{r}_w = \frac{r_w}{2}\left[\left(\frac{K_X}{K_Y}\right)^{1/4} + \left(\frac{K_Y}{K_X}\right)^{1/4}\right]. \tag{9}$$

The X and Y are axes of a new reference system, parallel to the principal directions of the permeability tensor, which in the Cartesian reference system is given by

$$\mathbf{K} = \begin{pmatrix} K_{xx} & K_{xy} \\ K_{xy} & K_{yy} \end{pmatrix}. \tag{10}$$

This new reference system is found considering a rotation of the Cartesian axes. In general, for a symmetric tensor given by Eq. (10), this rotation is defined by the angle

$$\alpha = \frac{1}{2}\arctan\left(\frac{2K_{xy}}{K_{xx} - K_{yy}}\right). \tag{11}$$

The tensor components of the new reference system are given by

$$K_X = K_{xx}\cos^2\alpha + K_{yy}\sin^2\alpha + K_{xy}\sin 2\alpha, \tag{12}$$

$$K_Y = K_{xx}\sin^2\alpha + K_{yy}\cos^2\alpha - K_{xy}\sin 2\alpha. \tag{13}$$

The problem just described also needs to be solved numerically in order to determine a well index value. Therefore, only a portion of the original reservoir grid will be considered.

It must contain the considered well and an appropriate number of cells, as exhibited in Fig. 3(b) [2]. In this auxiliary problem, it is considered a prescribed flow condition for the well and Dirichlet conditions on the boundary of the selected portion grid, whose values are determined through the analytical solution $P(x, y)$. For the auxiliary problem solution, the flow rate q, wellbore pressure P_w and mobility λ can be arbitrary values. Nonetheless, it is important that the permeability and the wellbore radius match the specified values employed to solve the problem in the whole reservoir.

With the auxiliary problem solution, two solutions for the pressure field are available, an analytical, given by Eq. (7), and a numerical. In general, these solutions will be significantly different, since the numerical one can not capture the high pressure gradient in the near-well region. The grid is not sufficiently refined for this. The flow rate value q, on the other hand, is the same on both solutions, since it was imposed on the numerical solution. Then, it is possible to apply the Eq. (2) and obtain the well index

$$\mathrm{WI} = \frac{q}{\lambda \left(P_p - P_w\right)}. \tag{14}$$

In the last equation, q, P_w and λ values should be those ones employed to solve the auxiliary problem. The pressure value P_p will be the discrete pressure obtained in the numerical solution. It is associated with the cell containing the well. The well index value obtained by Eq. (14) can be now applied to solve problems considering the whole grid, including problems with different operating conditions considered in the auxiliary problem.

The well index determined by the presented procedure takes into account not only the geometric characteristics of the grid surrounding the well, but also the permeability in this region, as well as the Peaceman well model. The main difference between them is that these data are indirectly included in the discretization method employed to solve the auxiliary problem. Consequently, it is important that the discretization method employed in the auxiliary problem is the same used to obtain the solution for the whole reservoir. Thus, the well index value will depend on, besides the local grid geometry and the permeability, the considered discretization method.

4 RESULTS

The main purpose of the numerical experiments presented in this section is to perform a comparison between the two possible alternatives to treat the well in the numerical formulation. The accuracy is quantified employing a reference solution. In the present case, this solution is a numerical one obtained in an extremely refined grid.

4.1 Grids considered

All grids employed in the numerical experiments have the structure and dimensions showed in Fig. 4. Theses grids, both for the approach 1 and approach 2, keep the transition and Cartesian portions fixed and present always 12 divisions in the circumferential direction in the polar portion. The transition region has 52 cells, while the Cartesian one has 176 cells.

[2] The described methodology is general. It can be applied to any unstructured grid, as depicted in Fig. 3(b). However, in the present case, the grid around the well will be always a polar grid.

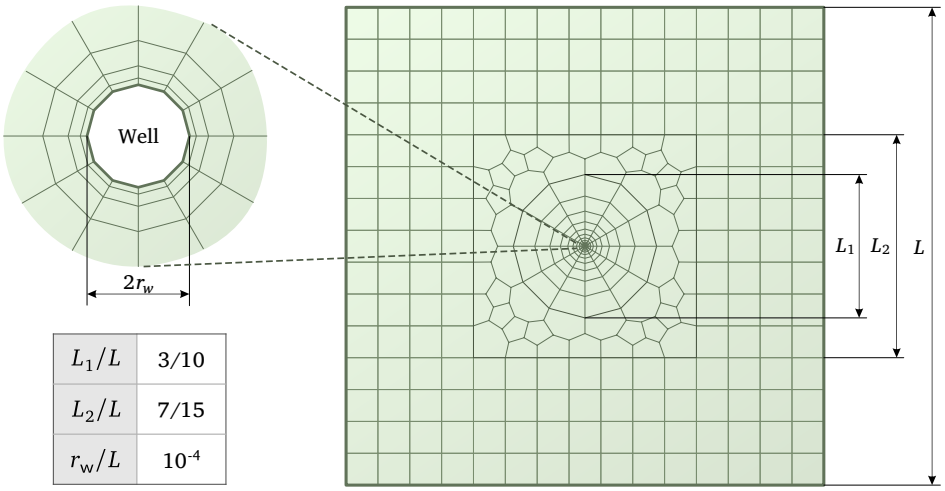

L_1/L	3/10
L_2/L	7/15
r_w/L	10^{-4}

Figure 4: Grids employed in the tests.

Regarding the approach 1, ten grids were considered in order to analyze the solution behavior as the polar grid refinement occurs. Their geometric characteristics are shown in Fig. 5, and the radial spacing of all polar grids obeys the exponential increasing defined in Eq. (1). It is important to notice that, employing this procedure to build the polar grid, only in the portion really near of the well there is an effective refinement. The cells adjacent to the transition portion have an approximately constant size.

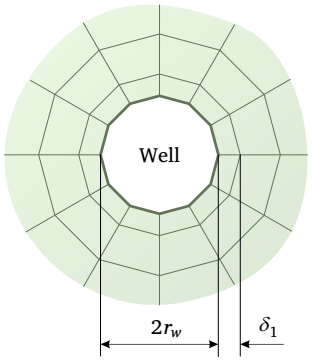

	δ_1/r_w	N_r	N_c
1	8.0	15	180
2	4.0	18	216
3	2.0	21	252
4	1.0	24	288
5	0.5	27	324

	δ_1/r_w	N_r	N_c
6	0.25	30	360
7	0.125	33	396
8	0.0625	36	432
9	0.03125	39	468
10	0.015625	42	504

Figure 5: Parameters of the polar grids employed in the tests related to approach 1 (N_r: number of divions in the radial direction, N_c: number of cells in the polar portion).

The polar portion, in the approach 2, is built differently than in approach 1. The major difference is that the wellbore surface is no longer represented as a boundary of the grid. Instead, there is a central cell which contains the well, as illustrated in Fig. 6. Moreover, as no high radial refinement is required, only a linear increase of the radial spacing was considered. The geometrical restrictions for the polar grid building in this approach are: the spacing δ_1 is two times the radius r_0 of the cell that contains the well, and the spacing near of the transition portion has a fixed value, $\delta_n/L = 0.045$.

The flow rate approach to/from the well is detached from the pressure gradient approach, when a well model is employed. Because of this, there should be no significant influence of the polar grid refinement level. Then, only three grids were considered for the tests considering approach 2. The geometric parameters of these grids are shown in Fig. 6.

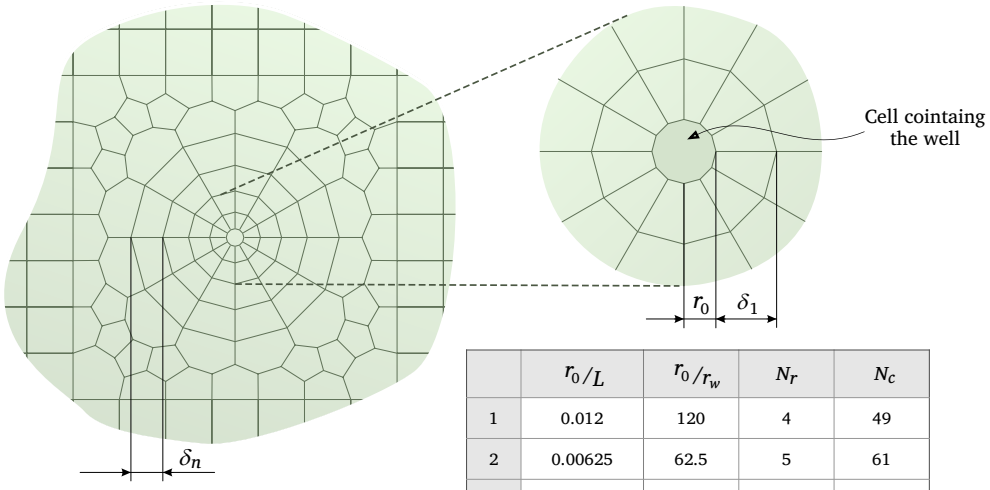

	r_0/L	r_0/r_w	N_r	N_c
1	0.012	120	4	49
2	0.00625	62.5	5	61
3	0.00214	21.4	6	73

Figure 6: Parameters of the polar grids employed in the tests related to approach 2 (N_r: number of divions in the radial direction, N_c: number of cells in the polar portion).

4.2 Problem specification

In order to evaluate the approaches described in sections 2 and 3, it was considered the incompressible single-phase flow problem illustrated in Fig. 7. A producing well is located in the center of the square domain, Dirichlet and Neumann conditions are prescribed in the boundaries and the variables values are normalized. The dimensionless pressure $\tilde{P}$ and velocity $\tilde{\mathbf{v}}$ shown in Fig. 7 are given, respectively, by

$$\tilde{P} = \frac{P - P_{\mathrm{w}}}{P_b - P_{\mathrm{w}}}, \tag{15}$$

$$\tilde{\mathbf{v}} = \frac{\mathbf{v}}{\dfrac{K_{min}}{\mu}\left(\dfrac{P_b - P_{\mathrm{w}}}{L}\right)}, \tag{16}$$

where P_b is the pressure prescribed on the top and left boundaries and K_{min} is the smallest eigenvalue of the $\mathbf{K}$ tensor. The associated dimensions are also normalized, considering in this case the domain dimension L.

Different permeability tensors were considered in the tests by varying the anisotropy ratio. The general expression to specify the permeability tensor is

$$\tilde{\mathbf{K}} = \begin{pmatrix} \cos\alpha & -\sin\alpha \\ \sin\alpha & \cos\alpha \end{pmatrix} \begin{pmatrix} 1 & 0 \\ 0 & R \end{pmatrix} \begin{pmatrix} \cos\alpha & \sin\alpha \\ -\sin\alpha & \cos\alpha \end{pmatrix}, \tag{17}$$

where α is the angle formed by the principal axes of the tensor and the Cartesian axes. The permeability tensor $\tilde{\mathbf{K}}$ is a dimensionless tensor whose definition is given by $\tilde{\mathbf{K}} = (1/K_{min})\,\mathbf{K}$. Additionally, R can be interpreted as the tensor anisotropy ratio.

The problem just defined will be solved considering the set of grids described in the last subsection. For approach 1, the $\tilde{P}_{\mathrm{w}}$ pressure is prescribed as a Dirichlet condition on the grid

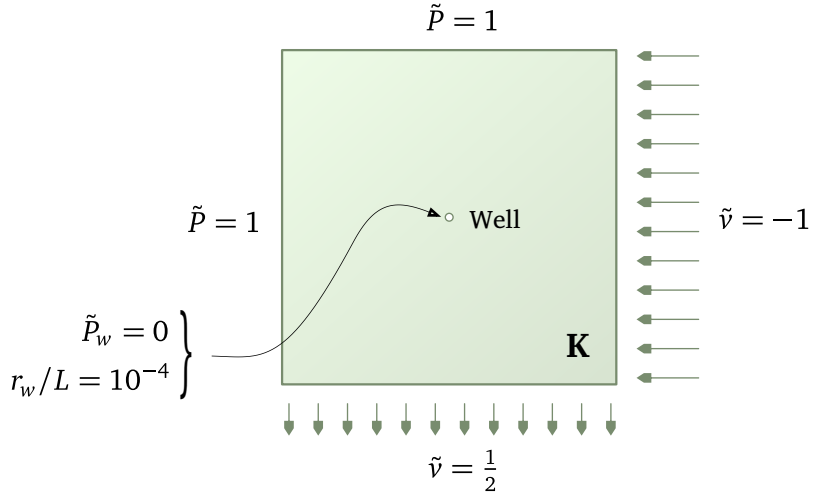

Figure 7: Boundary conditions for the single-phase fluid flow problem.

boundary representing the wellbore surface. The situation is different in the approach 2, since the wellbore surface is not represented as a boundary of the domain. For this case, $\tilde{P}_w$ pressure is imposed through the well model. However, in both cases, the unknown problem and the parameter to be compared is the flow rate leaving the domain through the well.

The numerical methodology employed to discretize the differential equation that models the incompressible single-phase fluid flow is CTPFA - corrected two-point flux approximation (Cerbato et al., 2014). It is a finite volume method able to deal with hybrid grids.

Unfortunately, an analytical solution for the mentioned problem is not available and, moreover, to build a manufactured solution compatible with the flow behavior in the vicinity of a well is extremely difficult. Because of this, it was decided to consider the numerical solutions in an extremely refined grid as reference solutions. This grid, shown in Fig. 8, has 116726 triangle cells, 58663 vertices and it is refined in the whole domain, specially in the vicinity of the well, where the refinement is more pronounced. The mentioned refinement is done in the radial and circumferential directions, differently than occur in the grids employed to test the approach 1. In addition, the wellbore surface is represented as a circular boundary of the refined grid, so, no well model will be used.

The reference solutions were determined through an independent code based on the EFVLib library (Maliska et al., 2009). The code employs the Element-based Finite Volume Method - EbFVM (Maliska, 2004, Cordazzo, 2006, Hurtado et al., 2007), in which the unknowns are associated to the vertices of the grid. In Fig. 9 there are the pressure fields obtained for three anisotropy levels, $R = \{1, 10, 100\}$, and a 30° angle. It is important to notice that these pressure fields do not have a radial symmetric from a certain distance of the well. For anisotropic cases, the highest pressure gradients are aligned with one of the principal directions of the permeability tensor, which is rotated 30° with respect to the vertical axis.

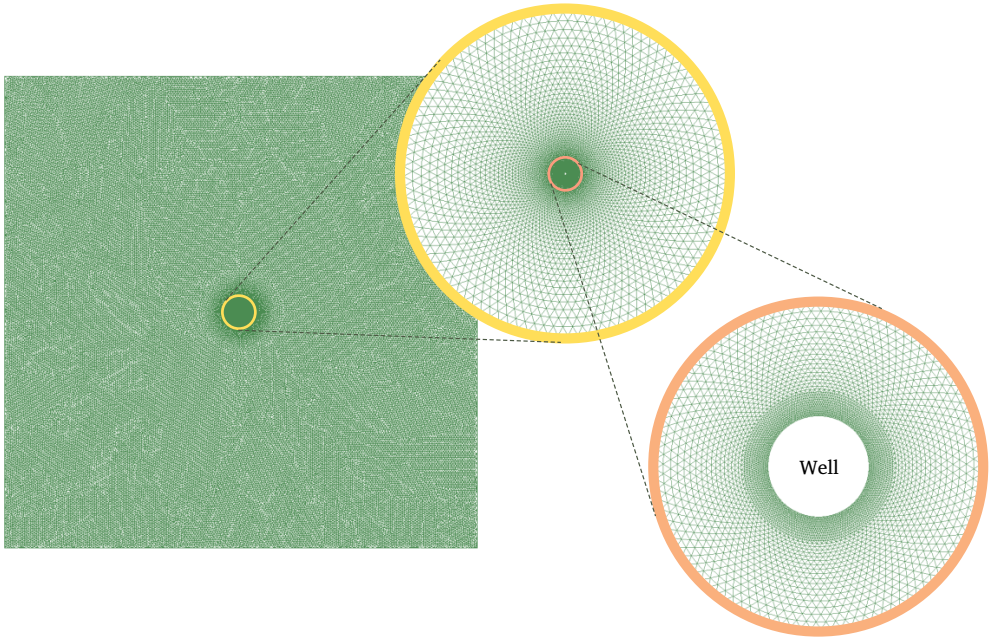

Figure 8: Refined grid employed to obtain the reference solutions.

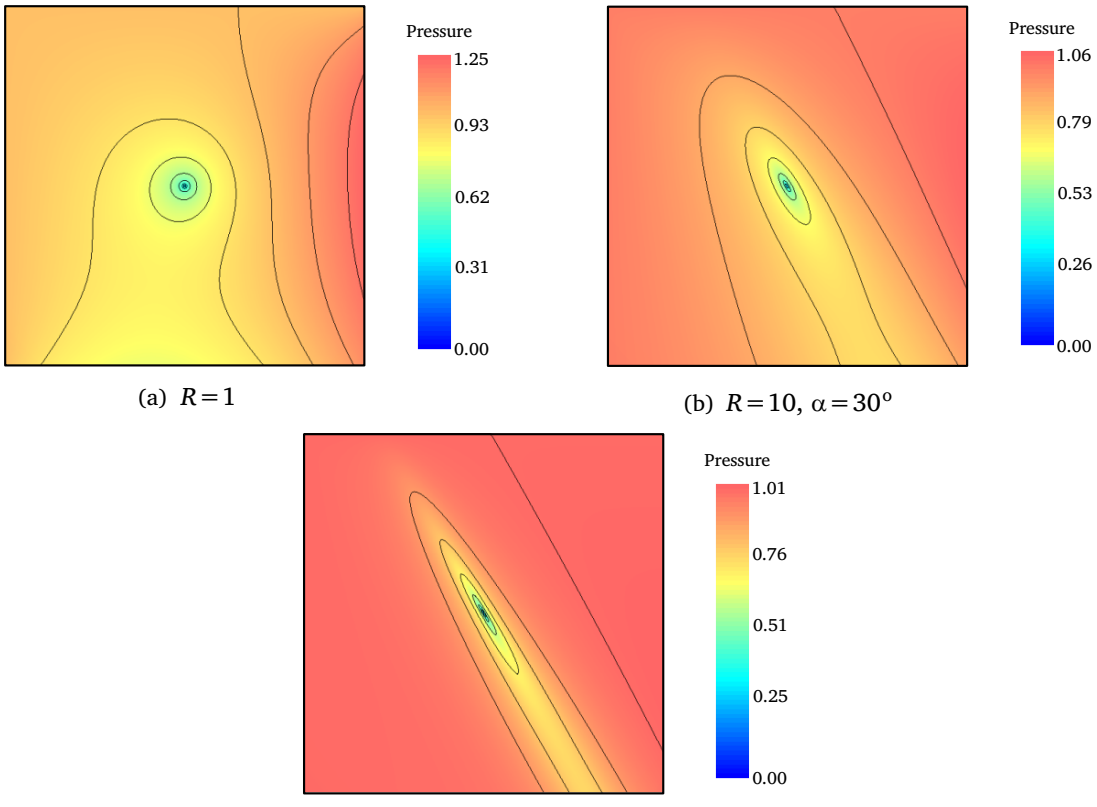

(a) $R=1$

(b) $R=10,\ \alpha=30^o$

(c) $R=100,\ \alpha=30^o$

Figure 9: Pressure fields in the reference solutions considering three anisotropy levels.

Finally, in Table 1 there are the flow rate values determined from the reference solutions employing the mentioned three anisotropy levels and the angle $\alpha = 30^o$. These values will be compared to those ones obtained when the approaches 1 and 2 are employed.

Table 1: Dimensionless flow rate values obtained in the reference solutions.

	R	$\tilde{\mathbf{K}}$	$\tilde{q}$
1	1	$\begin{pmatrix} 1 & 0 \\ 0 & 1 \end{pmatrix}$	0.7460
2	10	$\begin{pmatrix} 3.25 & -3.897 \\ -3.897 & 7.75 \end{pmatrix}$	2.2556
3	100	$\begin{pmatrix} 25.75 & -42.868 \\ -42.868 & 75.25 \end{pmatrix}$	8.4967

4.3 Results employing approach 1

As previously mentioned, in approach 1 no well model is considered. Instead, the wellbore surface is included as a boundary, where the pressure P_w is prescribed as Dirichlet condition. Although the grids employed are composed by portions with different topology, in all of these portions it was considered the same methodology to discretize the incompressible single-phase model (CTPFA).

The results obtained employing the set of 10 hybrid grids described in subsection 4.1 are shown in Fig. 10 for the isotropic case ($R = 1$). In this plot, the variation of the dimensionless flow rate $\tilde{q}$ is presented as the polar portion is refined, specially near of the well. The values reached employing the mentioned methodology are compared with the reference value corresponding to this case. Those values were determined by adding the flows crossing the faces coincident with the boundary that represents the wellbore surface.

As can bee seen in Fig. 10, the flow rates obtained with CTPFA method converge to a value very close to the reference one. It is possible to notice that, after a certain refinement level ($\delta_1/r_w \approx 0.2$), there is no significant variation of the flow rate. If the approach 1 is to be considered the appropriate procedure to treat the wells, a practical rule for refining grids would be the relation $\delta_1/r_w = 0.1$. This conclusion is based on the reported results and the next ones.

Flow rate values for anisotropic cases are displayed in the next two figures. The set of ten hybrid grids are also employed. An anisotropic ratio $R = 10$ was employed to produce the results corresponding to Fig. 11 and an anisotropic ratio $R = 100$ to generate Fig. 12. The purpose of the analysis is to determine how sensitive the flow rate values are to the increasing of permeability ratio R. As can be noticed, for these cases, the discretization method provided flow values that converge to values far away from the reference solutions.

In order to show more clearly the significant difference between the previous results and the reference results, in Fig. 13 this discrepancy is represented in a percentage form, employing a bar chart. Each bar represents the percentage difference between the flow rate,

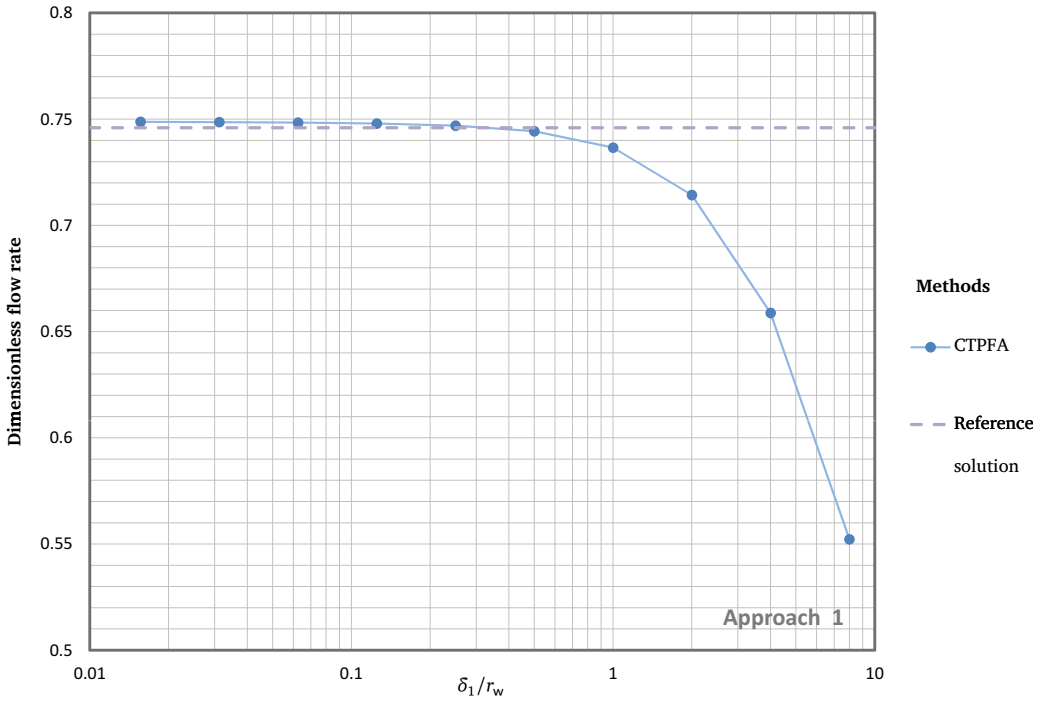

Figure 10: Flow rate values for an isotropic case employing approach 1.

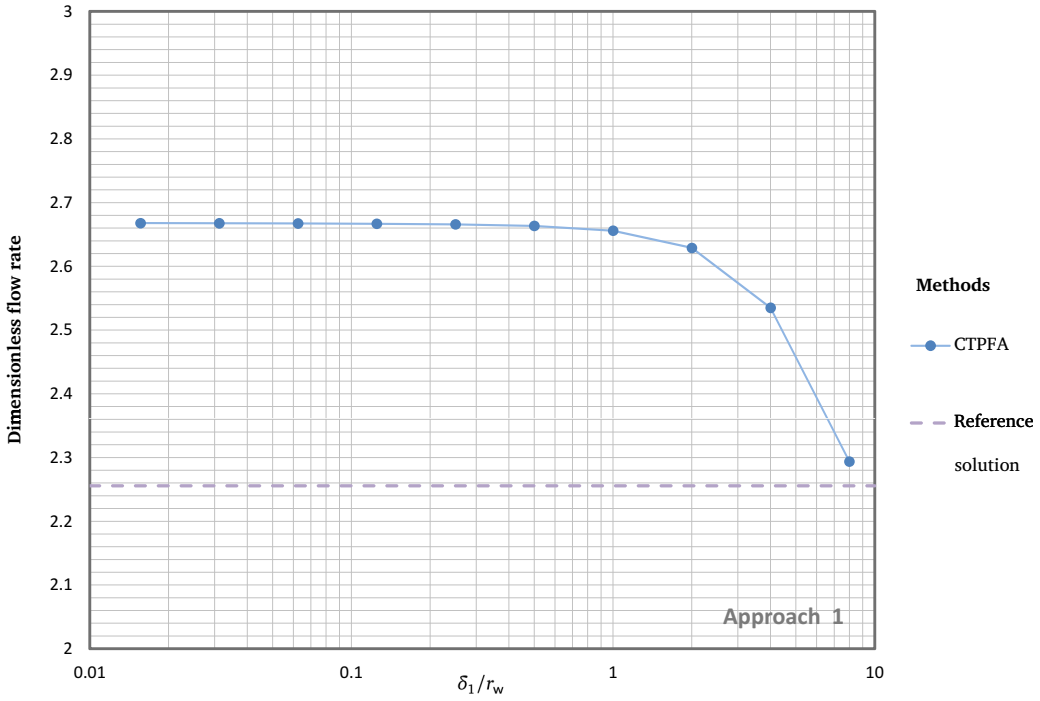

Figure 11: Flow rate values for an anisotropic case ($R = 10$ and $\alpha = 30^o$) employing approach 1.

obtained with CTPFA method in the most refined grid, and the corresponding reference solution. For the isotropic case, the discrepancy in the results is not evident. Unfortunately, this behavior is not noticed for anisotropic cases. The discrepancy level is unacceptable when the anisotropy ratio is $R = 100$. It is noteworthy that the approach 1 is not recom-

mended to treat the wells, unless for isotropic cases. The errors in the flow rate values grow significantly as the anisotropic ratio increases.

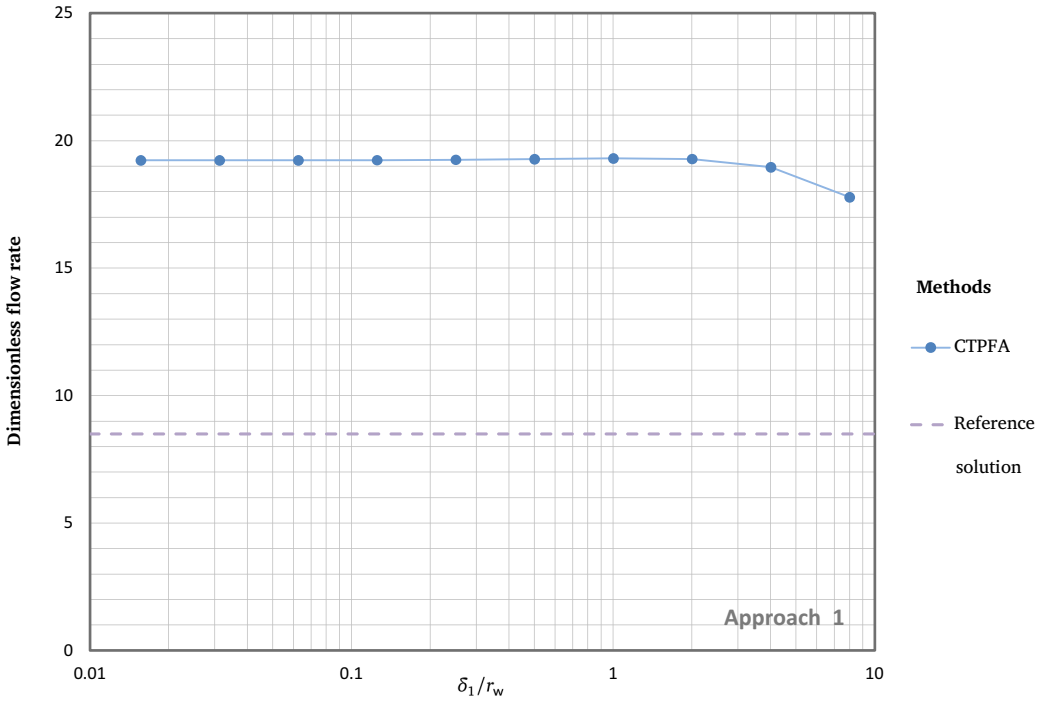

Figure 12: Flow rate values for an anisotropic case ($R = 100$ and $\alpha = 30^o$) employing approach 1.

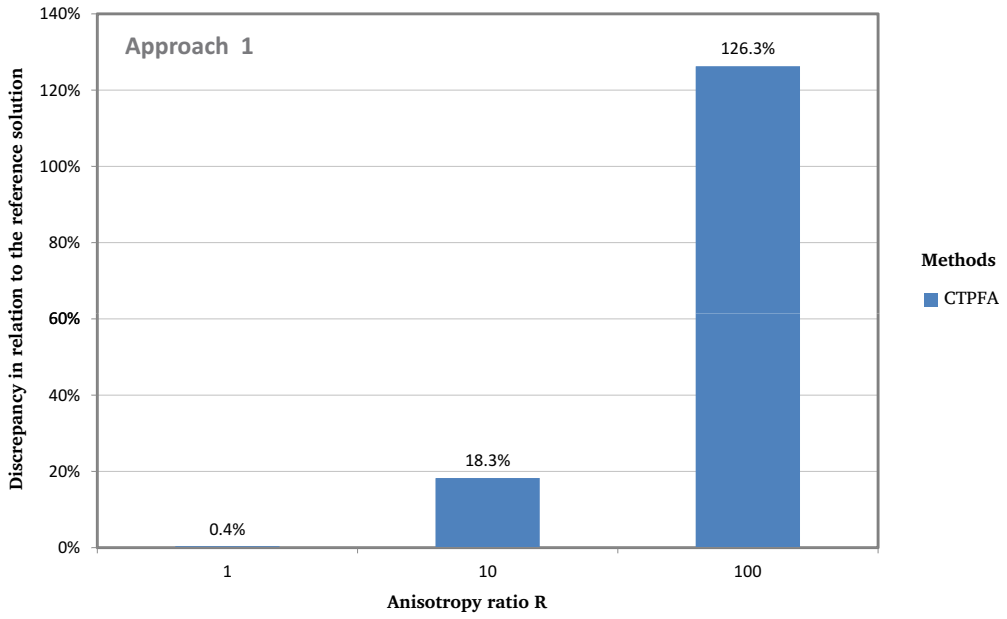

Figure 13: Discrepancy in the flow rate values comparing the solution obtained with approach 1 and the reference solution.

4.4 Results employing approach 2

The same numerical experiments described in subsection 4.3 were performed considering the approach 2, i.e., using a well model. In each case, the well indexes were determined according to the procedure described in subsection 3.1. It is important to emphasize that, for the determination of these well indexes, it was employed the same discretization method used to solve the fluid flow problem in the whole grid, since the well index depends on the discretization method. In other words, the fluid flow problem and the auxiliary problem, employed to determine the well index, are discretized by the CTPFA method.

Table 2 summarizes the results obtained for approach 2 employing the different grids presented in Fig. 6 and three anisotropy ratio levels. The first feature to be highlighted is the insensitivity of the flow rate values regarding the size of the cell containing the well. Although the radius of this cell in the grid 1 is one order of magnitude greater than the radius in grid 3, the flow rate values are almost the same, for a specific anisotropy ratio.

Table 2: Dimensionless flow rate determined by approach 2.

	Grid	CTPFA	Reference
R = 1	1	0.7448	0.7460
	2	0.7448	
	3	0.7448	
R = 10	1	2.2802	2.2556
	2	2.2798	
	3	2.2789	
R = 100	1	8.3200	8.4967
	2	8.3196	
	3	8.3166	

The discrepancy between the flow values displayed in Table 2 and the reference values is illustrated in Fig. 14. This figure is equivalent to Fig. 13, however, it should be noticed that the scales are different. Although the general trend is the same in both graphs, the anisotropy ratio increase is accompanied by a deterioration in the results, the discrepancy values with approach 2 are considerably lower to those ones observed in approach 1. The error levels are acceptable, including the case with $R = 100$.

It is possible that the error increase, in relation to the anisotropy ratio, is not only caused by some fault of the well model. The Fig. 9 shows that for the anisotropic cases, there are high pressure gradients relatively far away from the well. Probably, the poor representation of the solution employing the CTPFA method in this region contributes significantly to increase the error observed. This situation has no relation with the well model, but with the low grid refinement.

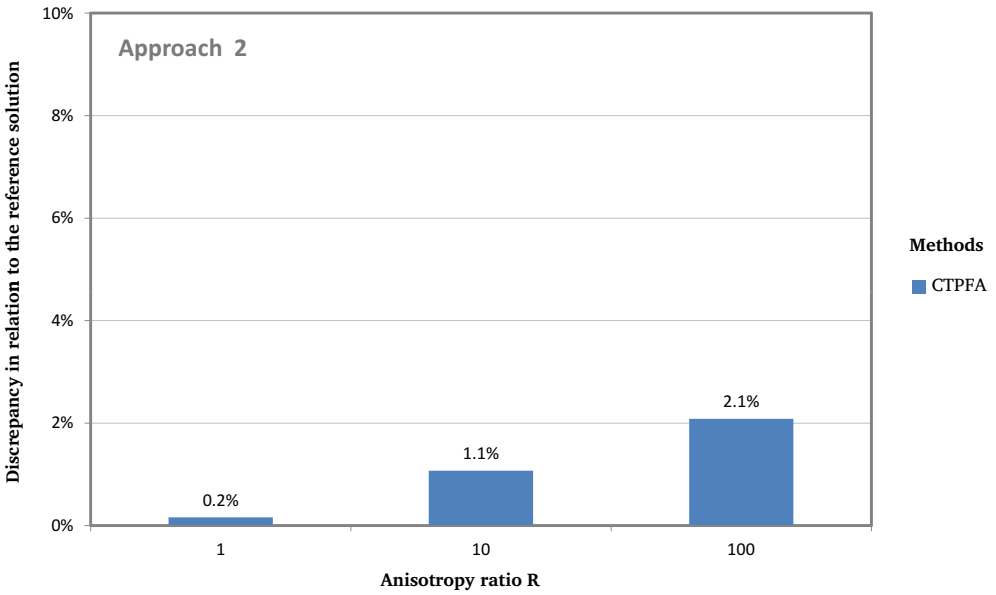

Figure 14: Discrepancy in the flow rate values comparing the solution obtained with approach 2 and the reference solution.

5 CONCLUSIONS

Two alternatives to treat the wells in reservoir simulation were presented in this paper. The first one employs a high grid refinement in the near-well region and recognizes the wellbore surface as an additional boundary of the problem. The other one is the most common alternative, the use of a well model. Some tests considering an incompressible single-phase flow problem were performed in order to compare the performance of those alternatives.

The approach 1 is a suitable alternative only for isotropic problems. In anisotropic problems, besides the pronounced gradient along the radial direction, there is a strong pressure variation in the circumferential direction near of the wellbore surface. It happens due to the elliptical shape of the pressure contours in theses cases. Apparently, to solve these problems in a proper manner, it is required to refine the polar grid also in the circumferential direction, at least where the circumferential derivative of the pressure is high. This alternative is not attractive because the grid generation would be linked to the permeability characteristics of the near-well region and it would increase the number of cells of the grid.

The alternative more reliable is the adoption of well models. Although the results show that the increment of the permeability ratio level reduces the accuracy to compute the flow rate, the error is within reasonable limits. As mentioned previously, it is likely that the flow rate error increasing is not only associated with a well model deficiency. In the numerical experiments, it was observed that the coarse grids away from the well could not properly capture the pressure variation, and this can have influenced the overall accuracy of the results. In general, the pressure field in anisotropic problems is much less smooth than in an isotropic case. So, it would be necessary a grid globally more refined to solve those problems in an appropriate way .

PERMISSION

The authors are the only responsibles for the printed material included in this paper.

ACKNOWLEDGEMENTS

This work was supported by the MaTra Project, granted by the Reservoir Simulation and Management Network (SIGER) and Petrobras.

REFERENCES

Aavatsmark, I. and Klausen, R. A. (2003). Well index in reservoir simulation for slanted and slightly curved wells in 3d grids. *SPE Journal*, 8:41–48.

Cerbato, G., Ribeiro, G. G., Hurtado, F. S. V., Maliska, C. R., and Silva, A. F. C. (2014). A method based on explicit gradient reconstruction applied to petroleum reservoir simulation. In *Proceedings of the XXXV Iberian Latin-American Congress on Computational Methods in Engineering*. CILAMCE 2014.

Cordazzo, J. (2006). Simulação de reservatórios de petróleo utilizando o método EbFVM e multigrid algébrico. Tese de doutorado, Departamento de Engenharia Mecânica, Universidade Federal de Santa Catarina, Florianópolis, Brasil.

Hurtado, F. S. V., Maliska, C. R., Silva, A. F. C., and Cordazzo, J. (2007). A quadrilateral element-based finite-volume formulation for the simulation of complex reservoirs. In *Proceedings of the X Latin American and Caribbean Petroleum Engineering Conference (LACPEC)*, Buenos Aires, Argentina.

Maliska, C. R. (2004). *Transferência de calor e mecânica dos fluidos computacional*. Editora LTC S. A., second edition.

Maliska, C. R., Silva, A. F. C., Hurtado, F. S. V., Donatti, C. N., and Pescador Jr., A. V. B. (2009). Desenvolvimento e implementação da biblioteca EFVLib. Relatório técnico SINMEC/SIGER I-03, parte 1, Departamento de Engenharia Mecânica, Universidade Federal de Santa Catarina.

Peaceman, D. W. (1978). Interpretation of well-block pressures in numerical reservoir simulation. *SPE Journal*, June 1978:183–194.

Peaceman, D. W. (1983). Interpretation of well-block pressures in numerical reservoir simulation with nonsquare grid blocks and anisotropic permeability. *SPE Journal*, June 1983:531–543.

Peaceman, D. W. (1990). Interpretation of well-block pressures in numerical reservoir simulation: Part 3 - off-center and multiple wells within a well-block. *SPE Journal*, May 1990:227–232.

Peaceman, D. W. (2003). A new method for calculating well indexes for multiple wellblocks with arbitrary rates in numerical reservoir simulation. In *SPE Reservoir Simulation Symposium*, Houston, Texas.